Mutual Interference of Multiple Surface Cracks Due to Rolling-Sliding Contact with Frictional Heating*

Takahito GOSHIMA** and Yuuji KAMISHIMA***

This paper deals with the two-dimensional rolling-sliding contact problem with frictional heat generation on an elastic half-space containing multiple surface cracks. Rolling-sliding contact is simulated as an arbitrarily distributed contact load with normal and shear components, moving with constant velocity over the surface of the half-space. The frictional heat generation at the region of contact is estimated by use of sliding velocity, frictional coefficient and contact pressure. Numerical results of stress intensity factors are obtained for the case of a set of parallel cracks due to Hertzian- and parabolic-distributed loads. The interferential effects on the stress intensity factors with the distance between two cracks, as well as the effects of the slide/roll ratio, frictional coefficient and crack angle, are considered.

Key Words: Elasticity, Thermal Stress, Stress Intensity Factor, Rolling-Sliding Contact, Mutual Interference, Surface Crack, Frictional Heating

1. Introduction

Since the analysis of Keer and coworkers[1),(2)], considerable research[(3)-(8)] on fracture mechanics has been performed for understanding the mechanism of the rolling contact fatigue failure in rail loads, gears and ball bearings. These studies, however, dealt with a single crack. In the actual rolling contact fatigue failure, multiple cracks occur. In the case of multiple cracks, Goshima and coworkers[(9),(10)] analyzed the stress intensity factors for multiple surface cracks in an elastic half-space under rolling contact, however, they only considered an isothermal case. Most rolling contacts are accompanied by frictional heat generation due to the relative slip between the two contact surfaces. Goshima and coworkers[(11)-(14)] have dealt with the thermoelastic rolling contact problem for a single surface crack. However, multiple crack analysis under rolling-sliding contact accompanied by frictional heating has not been performed as yet.

In this article, the stress intensity factors for multiple surface cracks in an elastic half-space under rolling-sliding contact loading accompanied by frictional heat are analyzed. Contact loading is simulated as a line contact pressure load with both normal and shear components having either Hertzian or parabolic distribution. The crack face friction is neglected. In the present temperature analysis, the speed of the moving contact region is assumed to be much greater than the ratio of the thermal diffusivity and the contact length (large Peclet number), and that the temperature distribution is not disturbed by the cracks. Numerical calculations of stress intensity factors are carried out for the case of a pair of parallel cracks. The effects of the distance between cracks, the frictional coefficient, the slide/roll ratio and the crack angle upon mutual interference of cracks are considered numerically.

2. Problem Formulation

An elastic half-space containing multiple surface cracks is subjected to rolling-sliding contact with constant moving velocity V as shown in Fig. 1. The

* Received 21st July, 1993. Paper No. 92-0236
** Faculty of Engineering, Toyama University, 3190 Gofuku, Toyama City 930, Japan
*** Toyama Murata Corporation, 345 Ueno, Toyama City 930, Japan

surface of the half-space is loaded by an arbitrarily distributed contact pressure $P_s(\tilde{x})$ and tangential frictional load $fP_s(\tilde{x})$ in the contact region (where f is frictional coefficient). Then, the frictional heat generation $Q_s(\tilde{x})$ is given as follows:

$$Q_s(\tilde{x})=fV_sP_s(\tilde{x}) \quad (1)$$

where V_s is the sliding velocity during rolling contact. In the analysis, the dimensionless parameters for the crack k are represented by subscript k (where $k=1, 2, \cdots, m$), and are shown as follows.

$$(x, y)=(\tilde{x}/c, \tilde{y}/c), (\xi_k, \zeta_k)=(\tilde{\xi}_k/c, \zeta_k/c)$$
$$x_k=\tilde{x}_k/c, x_k^*=\tilde{x}_k^*/c, d_k=\tilde{d}_k/c$$
$$P(x)=P_s(\tilde{x})/P_0, \iota_k=\tilde{\iota}_k/c, P_e=cV/\varkappa_t$$
$$S_r=V_s/V, H_0=2\alpha_0G_0\varkappa_t(1+\nu)/K_t(1-\nu) \quad (2)$$

where $\varkappa_t$ is thermal diffusivity, K_t is thermal conductivity, G_0 is shear modulus, ν is Poisson's ratio, α_0 is coefficient of thermal expansion, P_0 is the maximum pressure, P_e is Peclet number and S_r is slide/roll ratio.

The region outside the area of contact is assumed to be thermally insulated. Furthermore, it is assumed that the temperature distribution $T(x, y)$ is not affected by the presence of cracks. The thermal boundary conditions can now be given as follows.

$$\left(\frac{\partial T}{\partial y}\right)_{y=0}=\begin{cases} fcVS_rP_0P(x)/K_t, & |x|<1 \\ 0, & |x|>1 \end{cases} \quad (3)$$

$$(T)_{y\to-\infty}=0 \quad (4)$$

The mechanical boundary conditions on the surface and at infinity of the half-space are given as follows.

$$(\sigma_{yy})_{y=0}=\begin{cases} -P_0P(x), & |x|<1 \\ 0, & |x|>1 \end{cases} \quad (5)$$

$$(\sigma_{xy})_{y=0}=\begin{cases} fP_0P(x), & |x|<1 \\ 0, & |x|>1 \end{cases} \quad (6)$$

$$(\sigma_{pq})_{y\to-\infty}=0, (p, q=x, y) \quad (7)$$

Assuming that the crack face friction is neglected, the boundary condition along the cracks may be expressed as follows.

$$(\sigma_{\xi_k\zeta_k})_{\zeta_k=0}=0, 0<\xi_k<\iota_k, k=1, 2, \cdots, m \quad (8)$$
$$(\sigma_{\zeta_k\zeta_k})_{\zeta_k=0}=0, \xi_k\in\xi_{kop}, k=1, 2, \cdots, m \quad (9)$$

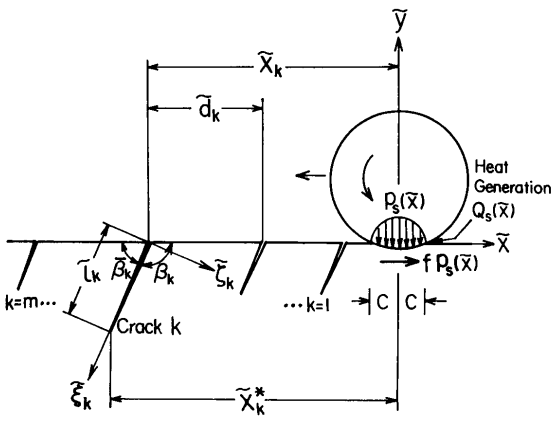

Fig. 1 Problem configuration and coordinate system

where ξ_{kop} is the crack face opening region of the crack k.

3. Stress Analysis

The stress field σ_{ij} is represented by superposition as:

$$\sigma_{ij}=\sigma_{ij}^0+\sigma_{ij}^1 (i, j=x, y \text{ or } \xi_k, \zeta_k). \quad (10)$$

Here σ_{ij}^0 denotes the stress in an uncracked half-space subjected to the rolling-sliding contact loading and heat generation in the contact region. The stress σ_{ij}^1 denotes the disturbance induced by the crack.

The solution of the stress σ_{ij}^0 which satisfies the boundary conditions Eqs. (3)-(7) is represented as follows[14]-[18].

$$\frac{\sigma_{ij}^0}{P_0}=\begin{cases} \int_{-1}^{1}P(t)F_{ij}dt, & x\leqq-1 \\ \int_{-1}^{x}P(t)G_{ij}dt+\int_{-1}^{1}P(t)F_{ij}dt, & -1<x\leqq1 \\ \int_{-1}^{1}P(t)G_{ij}dt+\int_{-1}^{1}P(t)F_{ij}dt, & x>1 \end{cases} \quad (11)$$

$$F_{ij}=(2\pi P_e)^{-1/2}\{(x-t)^2+y^2\}^{-3/4}H_0S_rfA_{ij}+2\{y+(2H_0S_r-1)(x-t)f\}B_{ij}\{(x-t)^2+y^2\}^{-2}/\pi$$
$$G_{ij}=0.5fS_rD_{ij}(\pi P_e)^{-1/2}(x-t)^{-5/2}e^{-P_ey^2/4(x-t)}$$
$$A_{xx}=\cos\theta_1+\sin\theta_1-1.5\cos\theta_0(\cos\theta_2+\sin\theta_2)$$
$$A_{yy}=\cos\theta_1+\sin\theta_1+1.5\cos\theta_0(\cos\theta_2+\sin\theta_2)$$
$$A_{xy}=1.5\cos\theta_0(\cos\theta_2-\sin\theta_2)$$
$$\theta_0=\tan^{-1}\frac{(x-t)}{y}, \theta_1=1.5\theta_0, \theta_2=2.5\theta_0$$
$$B_{xx}=(x-t)^2, B_{yy}=y^2, B_{xy}=-y(x-t)$$
$$D_{xx}=P_ey^2-2(x-t)-4P_e(x-t)^2$$
$$D_{yy}=2(x-t)-P_ey^2, D_{xy}=2y(x-t)P_e \quad (12)$$

To account for the disturbance σ_{ij}^1 caused by the crack, we consider the problem of multiple dislocations present at the points $z=z_{0k}$ ($z_{0k}=x_k+\eta_ke^{-i\beta_k}$ $k=1, 2, \cdots, m$) in an infinite space. Then the dislocation density is defined as:

$$\alpha_k=\frac{G_0\{[U_{\xi_k\xi_k}]+i[U_{\zeta_k\zeta_k}]\}e^{-i\beta_k}}{i\pi c(x+1)}, (k=1, 2, \cdots, m) \quad (13)$$

where $\{[U_{\xi_k\xi_k}]+i[U_{\zeta_k\zeta_k}]\}$ represent the displacement jumps. The solution to this problem is solved using the following complex potential functions[19].

$$\Phi_2(z)=\sum_{k=1}^{m}\left\{\frac{\alpha_k}{z-z_{0k}}\right\} \quad (14)$$

$$\Psi_2(z)=\sum_{k=1}^{m}\left\{\frac{\bar{\alpha}_k}{z-z_{0k}}+\frac{\alpha_k\bar{z}_{0k}}{(z-z_{0k})^2}\right\} \quad (15)$$

Then the stress representation is given by Muskhelishvili[20] as:

$$\sigma_{yy}+\sigma_{xx}=2\{\Phi_2(z)+\overline{\Phi_2(z)}\} \quad (16)$$
$$\sigma_{yy}-\sigma_{xx}-2i\sigma_{xy}=2\{z\overline{\Phi_2'(z)}+\overline{\Psi_2(z)}\} \quad (17)$$

where primes denote differentiation with respect to z ($=x+iy$). An additional potential, which is required

to remove the surface tractions, is conveniently written in terms of Φ_2, Ψ_2 as[20]:

$$\Phi_3(z)=\begin{cases}-\bar{\Phi}_2(z)-z\bar{\Phi}_2'(z)-\bar{\Psi}_2(z), & \mathrm{Im}(z)<0\\ \Phi_2(z), & \mathrm{Im}(z)>0.\end{cases} \quad (18)$$

Then the stress is expessed as follows[20].

$$\sigma_{yy}-i\sigma_{xy}=\Phi_3(z)-\Phi_3(\bar{z})+(z-\bar{z})\overline{\Phi_3'(z)} \quad (19)$$

Replacing the constant a_k by distributed dislocation density $a_k(\eta_k)d\eta_k$, defined along the line z_k of each cracks, the stress σ_{ij}^1 can be obtained by integration of η_k.

Substituting these results σ_{ij}^1 into Eq. (6) and the boundary conditions Eqs. (4) and (5), the following singular integral equations for a_k are obtained.

$$2e^{i\beta_k}\int_0^{l_k}\frac{a_k(\eta_k)}{\xi_k-\eta_k}d\eta_k+\sum_{j=1}^{m}\int_0^{l_j}\{a_j(\eta_j)C_{1k}(\xi_k,\eta_j)+\overline{a_j(\eta_j)}C_{2k}(\xi_k,\eta_j)\}d\eta_j=-(\sigma^0_{\zeta_k\zeta_k}-i\sigma^0_{\xi_k\zeta_k})_{\zeta_k=0},\quad (k=1,2,\cdots,m) \quad (20)$$

where

$$C_{1k}(\xi_k,\eta_j)=\hat{\Phi}_3(z_k;z_{0j})+(1-e^{2i\beta_k})\overline{\Phi_3^*(z_k;z_{0j})}-e^{2i\beta_k}\hat{\Phi}_3(\bar{z}_k;z_{0j})+e^{2i\beta_k}(z_k-\bar{z}_k)\overline{\Phi_3^{*\prime}(z_k;z_{0j})}+(1-\delta_{kj})L_{1k}(\xi_k,\eta_j) \quad (21)$$

$$C_{2k}(\xi_k,\eta_j)=\Phi_3^*(z_k;z_{0j})+(1-e^{2i\beta_k})\overline{\hat{\Phi}_3(z_k;z_{0j})}-e^{2i\beta_k}\Phi_3^*(\bar{z}_k;z_{0j})+e^{2i\beta_k}(z_k-\bar{z}_k)\overline{\hat{\Phi}_3^{*\prime}(z_k;z_{0j})}+(1-\delta_{kj})L_{2k}(\xi_k,\eta_j) \quad (22)$$

$$L_{1k}(\xi_k,\eta_j)=\Phi_2^*(z_k;z_{0j})+\overline{\Phi_2^*(z_k;z_{0j})}e^{2i\beta_k} \quad (23)$$

$$L_{2k}(\xi_k,\eta_j)=\overline{\Phi_2^*(z_k;z_{0j})}+\{z_k\Phi_2^{*\prime}(z_k;z_{0j})+\overline{\Psi_2^*(z_k;z_{0j})}\}e^{2i\beta_k} \quad (24)$$

$$\hat{\Phi}_3(z;z_0)=\begin{cases}-1/(z-\bar{z}_0), & \mathrm{Im}(z)<0\\ 1/(z-\bar{z}_0), & \mathrm{Im}(z)>0\end{cases} \quad (25)$$

$$\Phi_3^*(z;z_0)=\begin{cases}-(z_0-\bar{z}_0)/(z-z_0)^2, & \mathrm{Im}(z)<0\\ 0, & \mathrm{Im}(z)>0\end{cases} \quad (26)$$

$$\Phi_2^*(z;z_0)=1/(z-z_0) \quad (27)$$

$$\Psi_2^*(z;z_0)=\bar{z}_0/(z-z_0)^2 \quad (28)$$

$$\delta_{kj}=\begin{cases}1, & k=j\\ 0, & k\neq j\end{cases};\quad z_k=x_k+\xi_k e^{-i\beta_k}.$$

4. Numerical Calculations

Equation (20) was solved numerically using the piecewise quadratic method of Gerasoulis[21]. The singularity at the intersection of the crack and the free surface was assumed to be on the order of less than 0.5. This behavior was approximated numerically when $\tilde{a}_k(-1)=0$, where $\tilde{a}_k(\tilde{\eta}_k)$ is defined as:

$$a_k(\eta_k)=\frac{P_0\tilde{a}_k(\tilde{\eta}_k)e^{-i\beta_k}}{(1-\tilde{\eta}_k^2)^{1/2}},\quad \tilde{\eta}_k=\frac{2\eta_k}{l_k}-1. \quad (29)$$

Let us divide the interval $[-1,1]$ into $2N_k$ equal parts. We define the nodal points as $\tilde{\eta}_{k,n}=-1+(n-1)/N_k$ $(n=1\sim 2N_k+1)$, and use the Lagrange interpolation formula for three nodal points in the approximation. Setting the collocation points as $\xi_{k,r}=\eta_{k,r}+1/2N_k$ $(r$

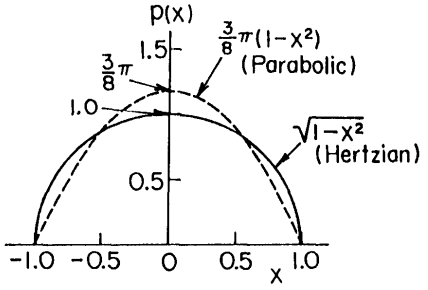

Fig. 2 Contact pressure distribution

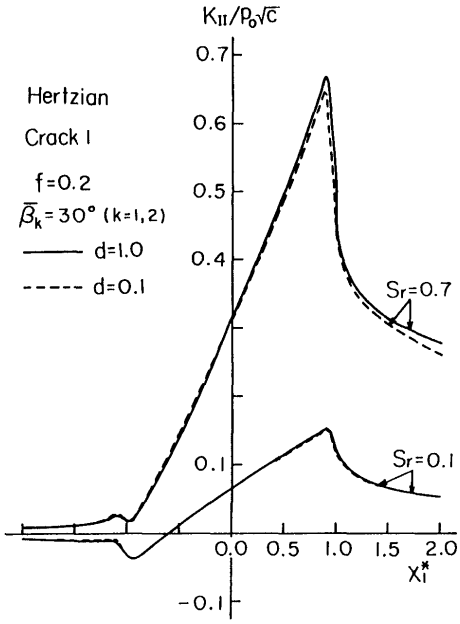

Fig. 3 Interferential effects on the variation of mode II stress intensity factors for crack 1 under Hertzian contact pressure distribution

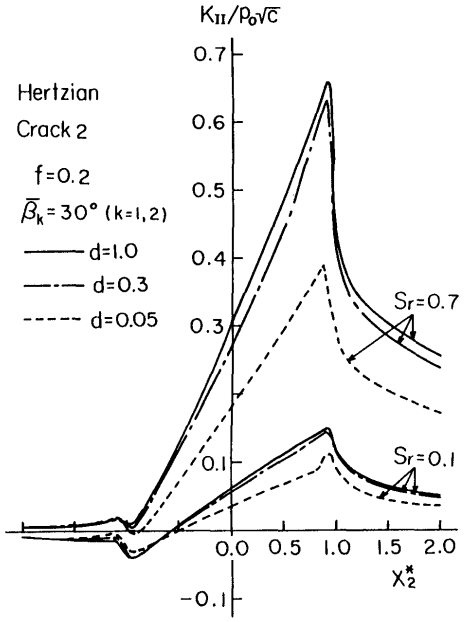

Fig. 4 Interferential effects on the variation of mode II stress intensity factors for crack 2 under Hertzian contact pressure distribution

$=1\sim 2N_k$), Eq. (20) reduces to the simultaneous linear algebraic system of $(2\sum_{k=1}^{m} N_k)$ equations for $\hat{a}_k(\hat{\eta}_{k,n})$. Using these solutions, the stress intensity factors for crack k are given as:

$$K_I - iK_{II} = \pi P_0 \sqrt{2\iota_k c}\, \hat{a}_k(1), (k=1, 2, \cdots, m). \quad (30)$$

In carrying out the numerical calculations, it was necessary to determine iteratively the degree of crack opening for a given set of parameters. Iteration was performed under the condition of the absence of overlap of the material. First, the numerical solution was obtained for a completely open crack (ξ_k^{op}: $0<\xi_k<\iota_k$ in Eq. (9)). The resulting crack opening displacement was checked by Eq. (13), and if overlap was found as $U_{\zeta_k\zeta_k}<0$, partial crack closure was approximated by setting $Re\{\hat{a}_k(\hat{\eta}_{k,n})\}=0$ over that portion of the crack where overlap occurred. Then the procedure was repeated for the partially closed crack and results were verified. This method generally converged within three iterations. With regard to the number of collocation points, a good accuracy was obtained for $N_k=10$.

Numerical calculations are carried out for the case of a pair of parallel cracks ($m=2$, $\beta_1=\beta_2$). We call these cracks crack 1 and crack 2 in the order of contact, and set the distance between these cracks as $d_k=d$. In the present calculations, the contact pressure $P(x)$ in Eq. (11) is given by Hertzian and

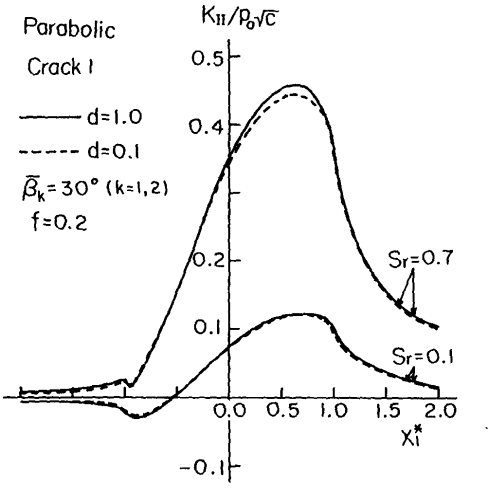

Fig. 5 Interferential effects on the variation of mode II stress intensity factors for crack 1 under parabolic contact pressure distribution

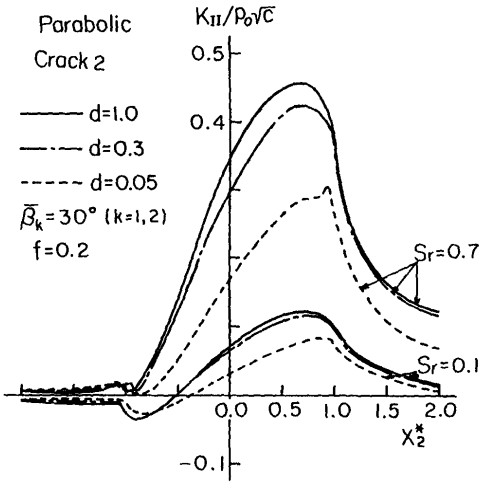

Fig. 6 Interferential effects on the variation of mode II stress intensity factors for crack 2 under parabolic contact pressure distribution

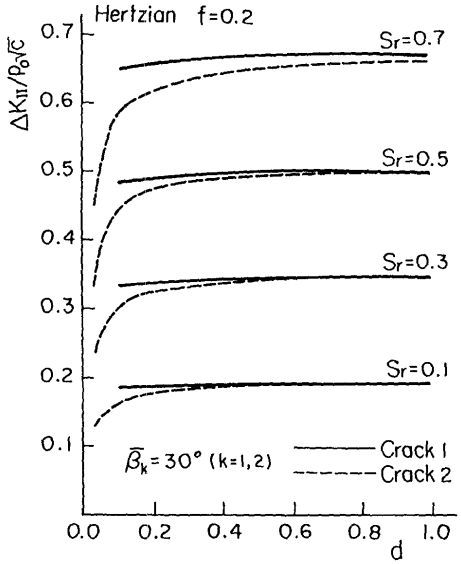

Fig. 7 Interferential effects on the range of mode II stress intensity factor ΔK_{II} under Hertzian contact pressure distribution for various values of slide/roll ratio

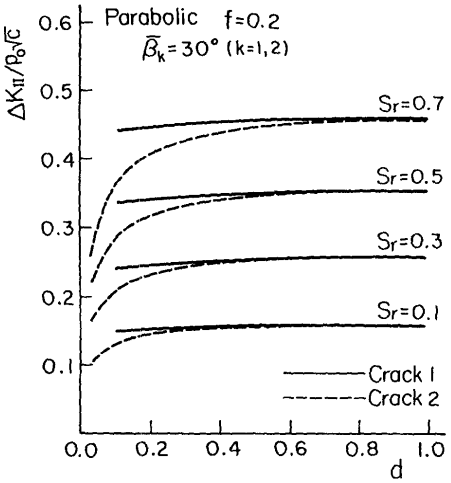

Fig. 8 Interferential effects on the range of mode II stress intensity factor ΔK_{II} under parabolic contact pressure distribution for various values of slide/roll ratio

parabolic distributions as shown in Fig. 2. Results are shown for the case of $\iota_1=\iota_2=0.1$, $P_e=100$ and $H_0=1.0$[22),(23)]. The numerical results of mode II stress intensity factors K_{II} of each crack are plotted as functions of the crack location over a complete loading cycle for Hertzian and parabolic cases in Figs. 3 and 4, and Figs. 5 and 6, respectively. These results are shown for the case of $f=0.2$, $\bar{\beta}_k=30°$ and $S_r=0.7$, 0.1, as the cracks approach each other until $d=0.1$ or 0.05. From these figures, we can evaluate the stress intensity factor range $\Delta K_{II}=(K_{II})_{max}-(K_{II})_{min}$, the results of which are shown in Figs. 7-10 as functions of the distance d between the cracks. From these figures, we can recognize the effect of mutual interference of the cracks; that is, the values of K_{II} and ΔK_{II} decrease with the approach of cracks, and these tendencies are more marked in crack 2 rather than crack 1. These interference effects become stronger for large slide/roll ratio (until $S_r=0.7$) and large frictional coefficient (until $f=0.8$). However, interference effects are not influenced very much by the difference between Hertzian and parabolic contact pressure distributions. In Figs. 3-6, the results for $d=1.0$ coincide with the results of the previous paper[14] for a single crack.

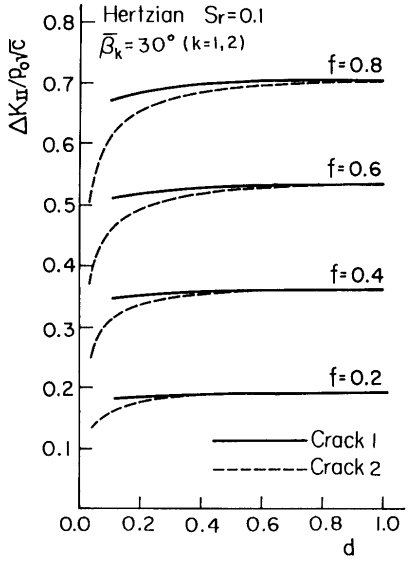

Fig. 9 Interferential effects on the range of mode II stress intensity factor ΔK_{II} under Hertzian contact pressure distribution for various values of frictional coefficients

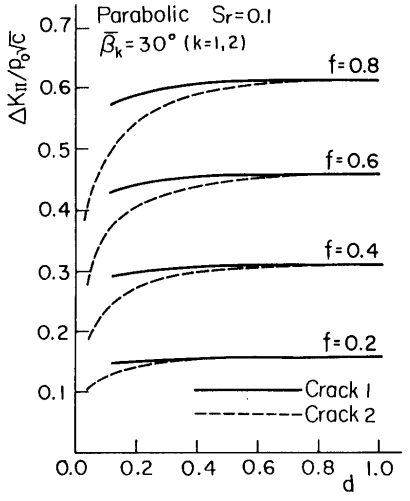

Fig. 10 Interferential effects on the range of mode II stress intensity factor ΔK_{II} under parabolic contact pressure distribution for various values of frictional coefficients

Figures 11 and 12 show the mode I stress intensity factors K_I of crack 1 and crack 2 as functions of the crack location for Hertzian and parabolic distributions, respectively. These results are shown for the case of $S_r=0.1$, $\bar{\beta}_k=30°$, $f=0.2$, 0.8 and $d=1.0$, 0.5, 0.3. From these figures, we can see that K_I for both cracks increases with an increase of the frictional coefficient f, and the decreases with the approach of cracks due to mutual interference effect. The magnitudes of f, S_r and contact pressure distribution are not affected very much by the interference effect on K_I. When crack 1 reaches the contact region ($x_1^*>-1.0$), the value of K_I for crack 2 increases discontinuously at $x_1^*\fallingdotseq-1.0$; this is due to the abrupt tractiondue to closure of crack 1.

Finally, in order to investigate the effects of the crack angle $\bar{\beta}_k$ on the stress intensity factors and on

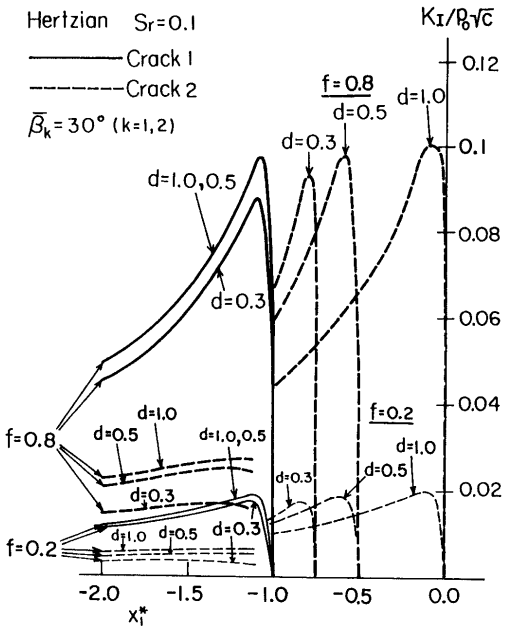

Fig. 11 Interferential effects on the variation of mode I stress intensity factors under Hertzian contact pressure distribution

their mutual interference, the numerical results of K_{II} and ΔK_{II} are shown for various values of d for the case of $S_r=0.1$, $f=0.2$ and Hertzian contact pressure distribution. Figures 13 and 14 show the variations of K_{II} as functions of crack location for cracks 1 and 2, respectively. The results are shown for $\bar{\beta}_k=20°$ and 60°. The maximum value of K_{II} for the shallow crack ($\bar{\beta}_k=20°$) is always larger than that for the deep crack ($\bar{\beta}_k=60°$), the former being affected significantly by contact load. Figure 15 shows ΔK_{II} as a function of the distance of cracks d at four values of $\bar{\beta}_k$. The interference effects for crack 2 are marked compared with crack 1, the latter being independent of $\bar{\beta}_k$. Figure 16 shows ΔK_{II} as a function of crack angle $\bar{\beta}_k$ at $d=1.0$, 0.1 and 0.05. From this figure, we can see that ΔK_{II} attains a maximum at $\bar{\beta}_k=30°\sim40°$ independent of the crack distance d.

5. Conclusions

This work has analyzed the stress intensity factors for multiple surface cracks due to rolling-sliding contact with frictional heat generation. From numerical examples of the stress intensity factors for a pair of parallel cracks, the following conclusions can be made.

(1) In the present numerical examples, magnitudes of mode I and mode II stress intensity factors decrease with decreasing distance between the two cracks due to the mutual interference by the cracks.

(2) The mode II stress intensity factors of crack

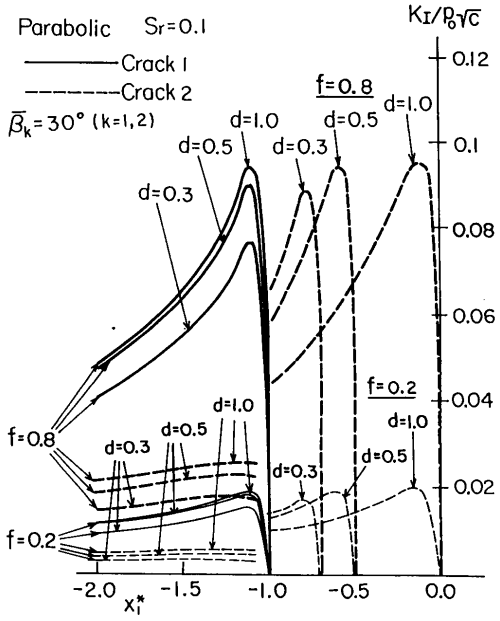

Fig. 12 Interferential effects on the variation of mode I stress intensity factors under parabolic contact pressure distribution

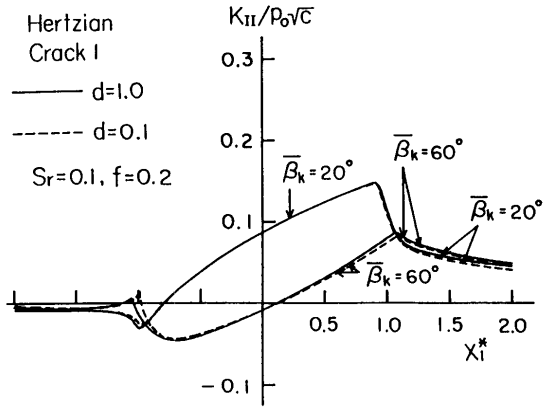

Fig. 13 Variation of mode II stress intensity factors for crack 1 under Hertzian contact pressure distribution for various crack inclination angles

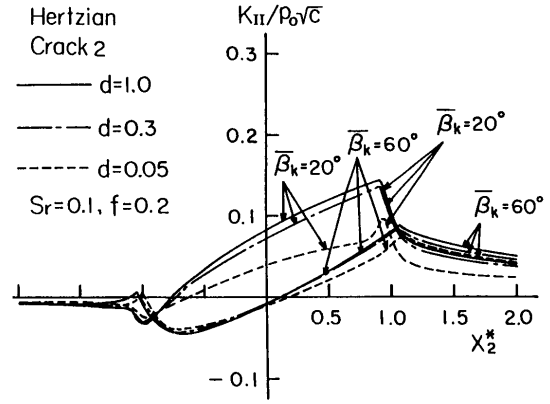

Fig. 14 Variation of mode II stress intensity factors for crack 2 under Hertzian contact pressure distribution for various crack inclination angles

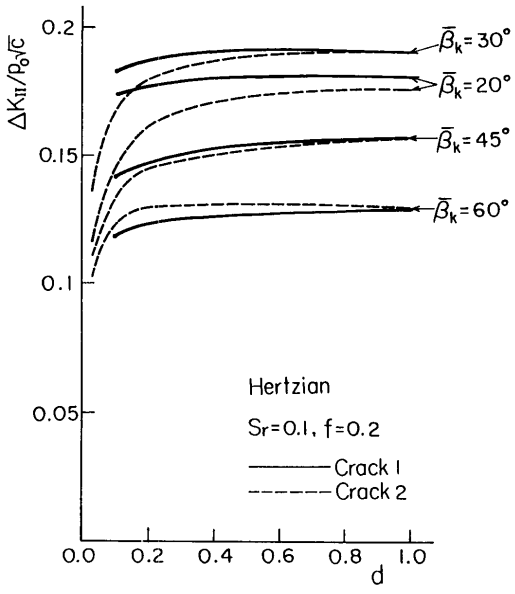

Fig. 15 Interferential effects on the range of mode II stress intensity factor ΔK_{II} under Hertzian contact pressure distribution for various crack inclination angles

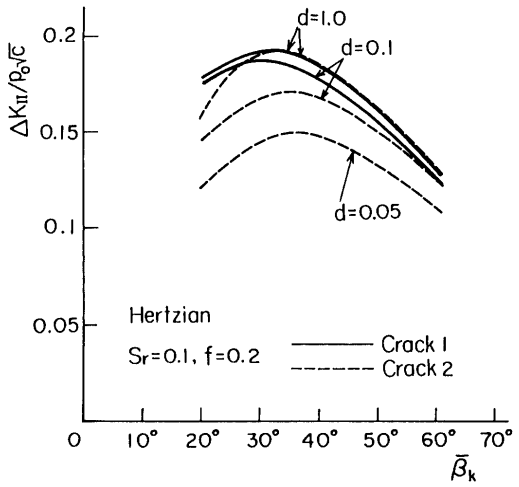

Fig. 16 Variation of the range of mode II stress intensity factor ΔK_{II} as a function of crack inclination angle under Hertzian contact pressure for various values of distance between the cracks

2 show a marked interference effect compared with crack 1, and these interference effects become stronger with the increase in the magnitude of slide/roll ratio or frictional coefficient; however, these effects are not influenced very much by the difference of contact pressure distribution and the crack inclination angle. On the other hand, the interference effects on mode I stress intensity factors are not influenced by the frictional coefficient and the contact pressure distributions.

(3) In the present numerical examples, when the crack inclination angle is 30°~40° the amplitude of the mode II stress intensity factor range attains a maximum independent of the crackdistance.

Acknowledgment

The authors wish to thank Professor L. M. Keer of Northwestern University for his helpful suggestions. The authors are also indebted to Mr. M. Takahashi who is a former student of Toyama University.

References

(1) Keer, L. M. and Bryant, M. D., A Pitting Model for Rolling Contact Fatigue, Trans. ASME J. Lubr. Technol., Vol. 105 (1983), p. 198.

(2) Bryant, M. D., Miller, G. R. and Keer, L. M., Line Contact Between a Rigid Indenter and a Damaged Elastic Body, Q. J. Mech. Appl. Math., Vol. 37 (1984), p. 467.

(3) Hearle, A. D. and Johnson, K. L., Mode II Stress Intensity Factors for a Crack Parallel to the Surface of an Elastic Half-space Subjected to a Moving Point Load, J. Mech. Phys. Solids, Vol. 33, No. 1, (1985), p. 61.

(4) Sheppard, S., Barber, J. R. and Comninou M., Short Subsurface Cracks under Conditions of Slip and Stick Caused by a Moving Compressive Load, Trans. ASME, J. Appl. Mech., Vol. 52 (1985), p. 811.

(5) Murakami, Y., Kaneta, M. and Yatsuzuka, H., Analysis of Surface Crack Propagation in Lubricated Rolling Contact, ASLE Trans., Vol. 28, (1985), p. 60.

(6) Kaneta, M., Murakami, Y. and Yatsuzuka, H., Mechanism of Crack Growth in Lubricated Rolling/Sliding Contact, ASLE Trans., Vol. 28, (1985), p. 407.

(7) Kaneta, M., Murakami, Y. and Yatsuzuka, H., Effects of Oil Pressure on Surface Crack Growth in Rolling/Sliding Contact, Tribology International, Vol. 20, (1987), p. 210.

(8) Bower, A. F., The Effects of Crack Face Friction and Trapped Fluid on Surface Initiated Rolling Contact Fatigue Cracks, Trans. ASME J. Tribol., Vol. 110, (1988), p. 704.

(9) Goshima, T., Miyao, K. and Kamishima, Y., Mutual Interference of Two Surface Cracks in a Semi-Infinite Body Due to a Rolling Contact, Trans. Jpn. Soc. Mech. Eng., (in Japanese), Vol. 57, No. 533, A (1991), p. 19.

(10) Goshima, T., Stress Intensity Factors of Multiple Surface Cracks on a Semi-Infinite Body due to Rolling-Sliding Contact, Trans. Jpn. Soc. Mech. Eng., (in Japanese), Vol. 58, No. 547, A (1992), p. 386.

(11) Goshima, T. and Keer, L. M., Thermoelastic Contact Between a Rolling Rigid Indenter and a Damaged Elastic Body, Trans. ASME J. Tribol., Vol. 112, (1990), p. 382.

(12) Goshima, T., Hanson, M. T. and Keer, L. M., Three-Dimensional Analysis of Thermal Effects on Surface Crack Propagation in Rolling Contact, J. Thermal Stresses, Vol. 13, (1990), p. 237.

(13) Goshima, T. and Miyao, K., Stress Intensity Factors of a Surface Crack in a Semi-Infinite Body due to Rolling-Sliding Contact and Transient Heating, Trans. Jpn. Soc. Mech. Eng., (in Japanese), Vol. 58, No. 547, A (1992), p. 393.

(14) Goshima, T. and Keer, L. M., Stress Intensity Factors of a Surface Crack in a Semi-Infinite Body due to Rolling-Sliding Contact and Frictional Heating, Trans. Jpn. Soc. Mech. Eng., (in Japanese), Vol. 56, No. 532, A (1990), p. 2567.

(15) Johnson, K. L., Contact Mechanics, (1984), p. 19, Cambridge University Press.

(16) Ling, F. F. and Mow, V. C., Surface Displacement of a Convective Elastic Half-Space Under an Arbitrarily Distributed Fast-Moving Heat Source, Trans. ASME J. Basic Eng., Vol. 87, (1965), p. 729.

(17) Mow, V. C. and Cheng, H. S., The Thermal Stresses in an Elastic Half-Space Associated with an

Arbitrarily Distributed Moving Heat Source, Z. Angew. Math. Phys., Vol. 18, (1967), p. 500.
(18) Ju, F. D. and Huang, J. H., Heat Checking in the Contact Zone of a Bearing Seal, Wear, Vol. 79, (1982), p. 107.
(19) Dundurs, J., Mathematical Theory of Dislocations, (1975), p. 70, ASME Publication.
(20) Muskhelishvili, N. I., Some Basic Problems in the Mathematical Theory of Elasticity, (1954), 4th Ed. Noordhoff.
(21) Gerasoulis, A., The Use of Piecewise Quadratic Polynomials for the Solution of Singular Integral Equations of Cauchy Type, Comput. Math. Applics., Vol. 8, (1982), p. 15.
(22) Azarkhin, A., Barber, J. R. and Rolf, R. L., Combined Thermal-Mechanical Effects in Frictional Sliding, Key Engineering Materials, Vol. 33, (1989), p. 135.
(23) Hills, D. A. and Barber, J. R., Steady Motion of an Insulating Rigid Flat-Ended Punch Over a Thermally Conducting Half-Plane, Wear, Vol. 102, (1985), p. 15